

Pericytes of Multiple Organs Do Not Behave as Mesenchymal Stem Cells In Vivo

Nuno Guimaraes-Camboa, Paola Cattaneo, Yunfu Sun, Thomas Moore-Morris, Yusu Gu, Nancy D. Dalton, Edward Rockenstein, Eliezer Masliah, Kirk L. Peterson, William B. Stallcup, et al.

▶ **To cite this version:**

Nuno Guimaraes-Camboa, Paola Cattaneo, Yunfu Sun, Thomas Moore-Morris, Yusu Gu, et al.. Pericytes of Multiple Organs Do Not Behave as Mesenchymal Stem Cells In Vivo. Cell Stem Cell, 2017, 20 (3), pp.345-359. 10.1016/j.stem.2016.12.006 . hal-01785316

HAL Id: hal-01785316
https://amu.hal.science/hal-01785316

Submitted on 4 May 2018

HAL is a multi-disciplinary open access archive for the deposit and dissemination of scientific research documents, whether they are published or not. The documents may come from teaching and research institutions in France or abroad, or from public or private research centers.

L'archive ouverte pluridisciplinaire **HAL**, est destinée au dépôt et à la diffusion de documents scientifiques de niveau recherche, publiés ou non, émanant des établissements d'enseignement et de recherche français ou étrangers, des laboratoires publics ou privés.

Author Manuscript

Author Manuscript

Author Manuscript

Author Manuscript

HHS Public Access

Author manuscript

Cell Stem Cell. Author manuscript; available in PMC 2018 March 02.

Published in final edited form as:

Cell Stem Cell. 2017 March 02; 20(3): 345–359.e5. doi:10.1016/j.stem.2016.12.006.

Pericytes of multiple organs do not behave as mesenchymal stem cells in vivo

Nuno Guimarães-Camboa[1,2], **Paola Cattaneo**[1], **Yunfu Sun**[3], **Thomas Moore-Morris**[4], **Yusu Gu**[5], **Nancy D. Dalton**[5], **Edward Rockenstein**[6], **Eliezer Masliah**[6], **Kirk L. Peterson**[5], **William B. Stallcup**[7], **Ju Chen**[5], and **Sylvia M. Evans**[1,5,8,*]

[1]Skaggs School of Pharmacy, University of California at San Diego, La Jolla, CA, 92093, USA

[2]Institute for Biomedical Sciences Abel Salazar and GABBA Graduate Program, University of Porto, Porto 4050-313, Portugal

[3]Key Laboratory of Arrhythmia, Ministry of Education, East Hospital, Tongji University School of Medicine, Shanghai, 200120, China

[4]INSERM UMRS 910, Aix-Marseille Université, Marseille, France

[5]Department of Medicine, University of California at San Diego, La Jolla, CA, 92093, USA

[6]Department of Neurosciences, University of California at San Diego, La Jolla, CA, 92093, USA

[7]Tumor Microenvironment and Cancer Immunology Program, Cancer Center, Sanford Burnham Prebys Medical Discovery Institute, La Jolla, CA, 92037, USA

[8]Department of Pharmacology, University of California at San Diego, La Jolla, 92093, CA, USA

Summary

Pericytes are widely believed to function as mesenchymal stem cells (MSCs) -multipotent tissue-resident progenitors with great potential for regenerative medicine. Cultured pericytes isolated from distinct tissues can differentiate into multiple cell types in vitro, or following transplantation in vivo. However, the cell fate plasticity of endogenous pericytes in vivo remains unclear. Here, we show that the transcription factor *Tbx18* selectively marks pericytes and vascular smooth muscle cells in multiple organs of adult mouse. FACS-purified *Tbx18*-expressing cells behaved as MSCs in vitro. However, lineage-tracing experiments using an inducible *Tbx18*-CreERT2 line revealed that pericytes and vascular smooth muscle cells maintained their identity in aging and diverse pathological settings, and did not significantly contribute to other cell lineages. These results challenge the current view of endogenous pericytes as multipotent tissue-resident progenitors, and

*Lead contact: Sylvia M. Evans (syevans@ucsd.edu)

Additional Resources: Author Contributions: N.G.-C., P.C., Y.S., T.M.-M., Y.G., N.D., and E.R. performed experiments. E.M. and W.B.S. provided essential reagents. N.G.-C. and S.M.E. conceived the study, analyzed data and wrote the paper. All authors discussed the results and commented on the manuscript.

The authors declare no competing financial interests.

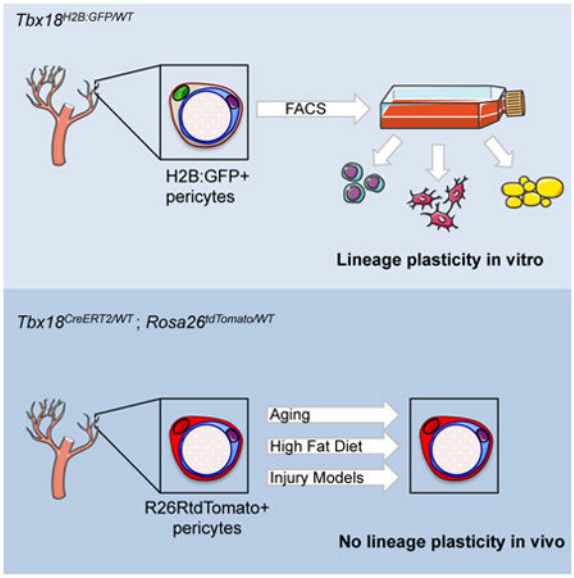
Publisher's Disclaimer: This is a PDF file of an unedited manuscript that has been accepted for publication. As a service to our customers we are providing this early version of the manuscript. The manuscript will undergo copyediting, typesetting, and review of the resulting proof before it is published in its final citable form. Please note that during the production process errors may be discovered which could affect the content, and all legal disclaimers that apply to the journal pertain.

Author Manuscript Author Manuscript Author Manuscript Author Manuscript

suggest that the plasticity observed in vitro or following transplantation in vivo arises from artificial cell manipulations ex vivo.

Graphical abstract

Guimarães-Camboa et al. permanently labeled pericytes and vascular smooth muscle of multiple organs in vivo and followed the fate of these cells in aging and injury models. Their analyses showed that, in vivo, pericytes did not behave as stem cells, challenging the current view of pericytes as tissue-resident multipotent progenitors.



Introduction

Most mammalian organs display a similar architecture (Figure S1A): a membranous cellular lining encapsulates a core of parenchymal cells supported by a stromal vascular fraction (SVF). The SVF is a heterogeneous group of cells, composed of immune cells, fibroblasts, endothelial cells, and mural cells (MCs). Mural cells comprise two cell types required to stabilize vascular networks: pericytes surround smaller caliber vessels, whereas vascular smooth muscle cells surround larger vessels (Armulik et al., 2011). Importantly, pericytes have been identified as Mesenchymal Stem Cells (MSCs): progenitors with capacity to attach to tissue culture plastic, that can be expanded in vitro for multiple passages, and induced to differentiate into osteogenic, chondrogenic or adipogenic lineages (Crisan et al., 2008). In vivo lineage tracing studies have reported pericytes as progenitors of white adipocytes (Tang et al., 2008), follicular dendritic cells (Krautler et al., 2012), and skeletal muscle (Dellavalle et al., 2011; Dellavalle et al., 2007). Pericytes have also been proposed to have the capacity to give rise to neurons, astrocytes and oligodendrocytes (Dore-Duffy et al., 2006), or to play a major role as fibroblast progenitors in fibrotic responses (Goritz et al., 2011; Greenhalgh et al., 2013).

Author Manuscript Author Manuscript Author Manuscript Author Manuscript

Owing to technological breakthroughs allowing for generation of induced pluripotent stem cells, it is currently possible to generate large numbers of patient-derived stem cells and differentiate them into specific cell types (Sancho-Martinez et al., 2012). However, clinical translation of this approach has proven extremely challenging, mainly due to genetic and epigenetic aberrations caused by in vitro culture, risk of tumorigenesis, and the lack of efficient strategies for cell delivery into certain solid organs (Ben-David and Benvenisty, 2011). Importantly, none of these limitations apply to tissue-resident progenitors. As such, boosting the potential of endogenous stem cells constitutes an attractive strategy for the development of new regenerative therapies. From this perspective, due to their broad distribution and reported multipotency, pericytes are considered to hold significant clinical potential. However, most reports claiming multipotency of pericytes are exclusively based on experiments performed utilizing cells cultured in vitro or on observations made in animals that received transplants of pericytes previously propagated in vitro. Importantly, artificial conditions and high concentration of mitogens that characterize cell culture systems may induce progenitor potential that may not be shared by the corresponding endogenous cells in vivo under physiological conditions (Snippert and Clevers, 2011).

Lineage tracing based on permanent genetic labeling constitutes the most reliable strategy to map the fate of any given cell population in vivo (Buckingham and Meilhac, 2011; Snippert and Clevers, 2011). Lineage tracing of pericytes has been previously performed using a constitutive *Pdgfrb*-Cre transgene (Foo et al., 2006; Krautler et al., 2012; Tang et al., 2008). Here we show that, although in adulthood PDGFRβ expression is largely restricted to pericytes and vascular smooth muscle, during embryogenesis PDGFRβ and the constitutive *Pdgfrb*-Cre allele are expressed in multiple cell lineages, rendering the latter unsuitable for tracking the progeny of mural cells. Notably, we have identified the *Tbx18* gene as being selectively expressed by all pericytes and vascular smooth muscle cells of specific organs in adult mouse, including retina, brain, heart, skeletal muscle, and white and brown fat depots. Following this expression profile, we generated a *Tbx18*-CreERT2 line that allowed for high-efficiency, time-controlled, genetic labeling of pericytes and vascular smooth muscle cells in intact tissues. This tool enabled us to track the progeny of pericytes during aging and in diverse pathological settings. Surprisingly, results from these experiments revealed that, in brain, heart, skeletal muscle, and fat, endogenous pericytes do not significantly contribute to other cell lineages. As a substantial number of experiments indicating that pericytes are MSCs have been performed on pericytes from these organs (Chen et al., 2015; Crisan et al., 2008; Dellavalle et al., 2011; Dellavalle et al., 2007; Paul et al., 2012; Tang et al., 2008), our results challenge the prevailing view of pericytes as multipotent tissue-resident progenitors.

Results

Tbx18 is expressed by pericytes and vascular smooth muscle

Major domains of *Tbx18* expression during embryogenesis have been previously described (Cai et al., 2008; Kraus et al., 2001), but little is known regarding *Tbx18* expression in adulthood. To investigate whether this gene was actively expressed in adult tissues, multiple organs were dissected from 8-week-old $Tbx18^{H2B\text{-}GFP/WT}$ mice (Cai et al., 2008) and processed for histological analyses. As displayed in Figure 1A-K, nuclear GFP fluorescence

Author Manuscript Author Manuscript Author Manuscript Author Manuscript

(previously shown to faithfully report active *Tbx18* expression (Cai et al., 2008)) was observed in interstitial cells of cardiac ventricles, skeletal muscle, all domains of brain, retina, white and brown adipose depots, bone marrow, inguinal lymph nodes, and skin. In addition to expression by numerous interstitial cells, robust GFP signal was also detected in smooth muscle of the aorta and ureters (Figure 1L, M) and in the membranous linings of several organs (pia mater, epicardium, pleura). In the heart, GFP fluorescence was also detected in pacemaker cells of the sino-atrial node (Figure 1N), a population known to be TBX18-dependent (Kapoor et al., 2013; Wiese et al., 2009). No detectable GFP signal was observed in kidney, gastro-intestinal tract or its accessory glands (Figure 1P-T).

We subsequently investigated the cell identity of interstitial *Tbx18*-expressing cells. Immunohistochemistry of brain, cardiac and skeletal muscle, brown and white fat depots using markers specifically recognizing highly-specialized cell types of these organs and the basement membrane marker Laminin, demonstrated that *Tbx18*-GFP+ interstitial cells did not correspond to parenchymal cells and were separated from these by a well defined basal lamina (Figure S1B). This observation placed interstitial *Tbx18*-GFP+ cells as components of the stromal vascular fraction.

Immunostaining with an anti-CD45 antibody demonstrated that interstitial *Tbx18*-GFP+ cells did not belong to the myeloid lineage (Figure S1C). Further analyses showed that *Tbx18*-GFP+ cells did not express the endothelial marker CD31/PECAM1, but were always located in the immediate vicinity of vascular endothelial cells, expressed the pan-pericyte marker CD140b/PDGFRβ, and had cytoplasmic projections enveloping smaller caliber vessels (Figure 2A). In the vicinity of larger arterioles and arteries, *Tbx18*-GFP+ cells were spindle-shaped, and expressed markers of vascular smooth muscle (Figure 2B). The vast majority of interstitial *Tbx18*-GFP+ cells were negative for the fibroblast marker CD140a/PDGFRα, with the exception of a very small subset of Tbx18-GFP+ cells, mainly in the vicinity of large vessels (Figure S2G-L). Interstitial *Tbx18*-GFP+ cells expressed CD146 (a marker of mural cells and endothelium, Figure S2A-F) as well as the pericyte and vascular smooth muscle marker NG2 (Figure S2G-L). Additional histological analyses using markers frequently used for the isolation of tissue-resident progenitors (Figure S3) allowed us to define a generic cell surface antigen profile of interstitial *Tbx18*-expressing cells of brain, retina, cardiac ventricles, skeletal muscle and fat depots as: CD31-, CD34-, CD45-, CD117-, Sca1-, CD29+, CD140b+, CD146+, NG2+ (Table S1).

Distribution, morphology and cell surface antigen signatures unequivocally identified interstitial *Tbx18*-GFP+ cells of fat depots, central nervous system and cardiac and skeletal muscle as pericytes and vascular smooth muscle. Immuno-gold electron microscopy analyses confirmed the identity of *Tbx18*-GFP+ cells as mural cells, including pericytes (Figure S2M). Importantly, in these organs, *Tbx18*-GFP expression did not mark a subset of mural cells, but rather labeled all pericytes (defined as PDGFRβ+, CD146+ double-positive cells, Figure 2C and S3Q) and vascular smooth muscle cells (identified as αSMA+ cells, Figure 2D). Moreover, our analyses revealed that, in such organs, all perivascular *Tbx18*-GFP+ cells were pericytes or vascular smooth muscle cells, as they always expressed markers of pericytes or vascular smooth muscle. However, we cannot exclude that other

Author Manuscript Author Manuscript Author Manuscript Author Manuscript

perivascular mesenchymal lineages might express *Tbx18* at levels below our threshold of detection.

Tbx18+ pericytes behave as MSCs in vitro

Based on the membrane antigen profile of mural cells (Table S1), we established a FACS protocol that, using *Tbx18*-H2B:GFP fluorescence and two fluorophore-conjugated antibodies recognizing CD146 and CD31, allowed for isolation of highly purified populations of pericytes/vascular smooth muscle, and endothelium from multiple tissues (Figure S4A, B). Utilizing this protocol, we isolated pericytes/vascular smooth muscle cells from peri-gonadal white adipose depots of $Tbx18^{H2B\text{-}GFP/WT}$ animals. These cells could be kept in culture for longer than six months (23 passages), retaining expression of *Tbx18* and mesenchymal markers (Figure S4C). Interestingly, *Tbx18* expression levels were considerably lower than those observed in vivo and detection of the nuclear signal from the *Tbx18*-H2B:GFP allele required the use of an anti-GFP antibody. Recent studies revealed that sustained *Tbx18* expression depends on short- range signals from neighboring cells (Bohnenpoll et al., 2013) and it is possible that the observed *Tbx18* downregulation is a consequence of removing these cells from their endogenous niche. In keeping with the reported plasticity of pericytes in vitro, when cultured in the appropriate media, *Tbx18*+ cells could differentiate into fat, bone, and cartilage, as expected from MSCs (Figure S4D-F). These observations confirmed that cultured *Tbx18*-GFP+ pericytes/vascular smooth muscle cells behaved as MSCs in vitro. However, they did not address whether these cells would exhibit similar properties in their in vivo niche (Snippert and Clevers, 2011).

Pdgfrb-Cre is not suitable for specific lineage tracing of mural cells

A substantial amount of in vivo evidence placing pericytes as tissue-resident progenitors is derived from genetic lineage tracing experiments using the *Pdgfrb*-Cre mouse line, in which expression of a constitutive Cre is under the control of a fragment of the *Pdgfrb* promoter (Foo et al., 2006). In adult animals PDGFRβ expression is confined to pericytes, vascular smooth muscle and a restricted subset of other stromal lineages (Armulik et al., 2011). However, during embryogenesis, PDGFRβ is broadly expressed throughout the embryo (Figure 3A). We have found that *Pdgfrb*-Cre extensively labels multiple cellular lineages from early developmental timepoints (Figure 3A). *Pdgfrb*-Cre labels embryonic hemogenic endothelium and produces extensive labeling of hematopoietic lineages in adult animals (90% of bone marrow cells, versus 96% labeled by *Tie2*-Cre, Figure 3B). Extensive labeling was also observed in adult kidney, lungs, skeletal muscle and brain (Figure 3C). These patterns of widespread labeling cannot be accounted for by transdifferentiation of pericytes into other cellular lineages and highlight the unsuitability of *Pdgfrb*-Cre for selective cell fate tracing of mural cells, including pericytes.

Pericytes maintain cell identity during aging

To specifically test the in vivo progenitor potential of pericytes, we generated an engineered *Tbx18* allele in which a Cre-ER^{T2} cassette, encoding a tamoxifen-inducible variant of Cre recombinase, was inserted 8 base-pairs downstream of the start codon (Figure 4A). Intra-peritoneal administration of 1 mg of tamoxifen to adult (8-week-old) $Tbx18^{CreERT2/Wt};Rosa26^{tdToma/Wt}$ animals for 3 consecutive days (Figure 4B) produced

Author Manuscript Author Manuscript Author Manuscript Author Manuscript

robust and reproducible labeling of more than 90% of pericytes and 85% of vascular smooth muscle in brain, heart, brown and white fat depots (Figure 4C,D and S5). Importantly, immunohistochemistry for Cre recombinase at time zero revealed that, in *Tbx18*-CreERT2; tdTomato-labeled pericytes, CreERT2 protein was localized to the nucleus. However, in non tdTomato-labeled pericytes, CreERT2 protein, despite being present at levels comparable to those of tdTomato-labeled cells, was not localized to the nucleus. These observations demonstrated that absence of tdTomato-labeling in a small fraction of mural cells (5 to 10% of pericytes, and 10 to 15% of vascular smooth muscle cells, depending on the tissue being considered, Figure 4C,D) reflected lack of *Tbx18*-CreERT2 activation in this small fraction of *Tbx18*-CreERT2 expressing cells, rather than constituting evidence for the existence of a *Tbx18*- or *Tbx18*^{low} subset of mural cells. *Tbx18*-CreERT2 also produced extremely efficient labeling of the membranous linings of the brain and heart, pia mater and epicardium, respectively. These labeling patterns completely mirrored domains of active *Tbx18* expression observed using the *Tbx18-H2B:GFP* allele. To investigate whether pericytes serve, during aging, as tissue resident progenitors that transdifferentiate into distinct cell lineages, organs were collected from *Tbx18*$^{CreERT2/Wt}$;*Rosa26*$^{tdToma/Wt}$ animals 8 and 87 weeks post-induction. Surprisingly, analysis of brain, heart, skeletal muscle, brown and white adipose depots revealed that *Tbx18*-CreERT2 lineage traced cells retained PDGFRβ expression throughout the experimental time course and did not significantly contribute to other cell lineages. In brain, lineage traced cells did not co-localize with neuronal or glial markers (Figure 4E-G; 3 animals per timepoint, 12 histological sections per animal), and in the heart, lineage traced cells did not co-localize with cardiomyocyte markers (Figure 4H-J; 3 animals per timepoint, 12 histological sections per animal). In distinct fat depots, labeled adipocytes were extremely rare, (less than 0.01%), similar to labeling frequencies observed at time-zero (3 animals per timepoint, 12 histological sections per animal, Figure 4K-P). Absence of trans-differentiation of pericytes contradicted the expectation that pericytes are multipotent tissue-resident progenitors that can contribute multiple cell types toward organ homeostasis during aging.

Pericytes are not adipocyte progenitors

Pericytes have been designated a source of white adipocyte progenitors (Tang et al., 2008) and recent reports suggested that at least a subset of beige adipocytes is derived from smooth muscle (Long et al., 2014). In this context, the clinical importance of mural cells is not associated with tissue regeneration, but rather is linked to obesity and associated metabolic disorders, being a cell type to target to prevent excessive production of new fat-storing cells. Lineage tracing using *Pdgfrb*-Cre and in vitro differentiation experiments were the basis of previous reports suggesting pericytes as adipocyte progenitors (Tang et al., 2008). However, as shown in Figure 3, *Pdgfrb*-Cre is unsuitable for pericyte-specific lineage tracing. Our pulse-chase studies using the *Tbx18*-CreERT2 allele suggested that neither pericytes or vascular smooth muscle had the potential to directly contribute to adipocytes during aging (Figure 4K-P). Animals utilized in these experiments were maintained on a lean diet, and we wondered whether manifestation of the adipogenic potential of pericytes might require a strong adipogenic stimulus. To test this, we subjected *Tbx18*$^{CreERT2/Wt}$;*Rosa26*$^{tdToma/Wt}$ animals to a high fat regimen. Animals were induced with tamoxifen at 8 weeks of age, and subsequently transferred to a high-fat diet. After six weeks of treatment, animals were

Author Manuscript Author Manuscript Author Manuscript Author Manuscript

euthanized and relevant fat depots were harvested for histological analyses (Figure 5A). As expected, this diet was a strong adipogenic stimulus, with high fat chow fed mice displaying a 29% increase in body weight over the six-week period versus a 12% increase in body weight for lean chow fed controls (Figure 5B). High-fat diet treated mice displayed enlarged adipose depots and hepatic steatosis (Figure 5C).

To investigate whether lineage traced pericytes or vascular smooth muscle had converted into lipid-storing cells, histological sections from three major fat depots (interscapular brown, perigonadal white, and inguinal white) were immunostained using an anti-Perilipin antibody to unequivocally identify adipocytes. As a positive control for adipocyte labeling by tdTomato, sections of similar tissues isolated from *Pdgfrb*-Cre*:Rosa26*$^{tdTomato/Wt}$ animals kept on lean chow were used. As observed in Figure 5D-F, *Pdgfrb*-Cre labeled the majority of adipocytes, regardless of the fat depot considered. On the other hand, as shown in Figure 5G-L, in the three types of fat depots analyzed, *Tbx18*-CreERT2 lineage traced cells did not colocalize with the adipocyte marker Perilipin, except for extremely rare events that occurred at a frequency similar to that observed at time zero (less than 0.01% of adipocytes labeled, 4 animals, 16 histological sections per animal), but rather retained PDGFRβ expression (Figure 5M-O), revealing that these cells had maintained their pericyte or vascular smooth muscle cell phenotype throughout the timecourse of the experiment. These results indicated that even under a strong adipogenic stimulus, adult pericytes and vascular smooth muscle cells did not transdifferentiate into adipocytes, challenging recent studies placing pericytes and vascular smooth muscle as progenitors of white and beige adipocytes, respectively (Long et al., 2014; Tang et al., 2008).

Pericytes are not fibrogenic or myogenic progenitors

Most mammalian organs react to mechanical or biochemical stress by eliciting a fibrotic response characterized by accumulation of fibroblasts secreting high amounts of extracellular matrix (ECM). This response is initially protective by nature, but excessive or permanent fibrosis can constitute a severe limitation to tissue regeneration and limit organ function. Recent studies have suggested that pericytes are the major precursor of fibroblasts in fibrotic responses (Greenhalgh et al., 2013). However, well-defined and pericyte-specific lineage tracing studies are required to determine the extent of this contribution.

We used the pericyte-labeling properties of *Tbx18*-CreERT2 to investigate whether pericytes within heart gave rise to fibroblasts in a model of fibrosis induced by trans-aortic constriction (TAC) (Rockman et al., 1991). To unequivocally monitor fibroblasts actively depositing ECM within the fibrotic scar, we performed these experiments in animals carrying a *Col1a1*-GFP transgene that functions as a faithful fibroblast marker in multiple organs (Moore-Morris et al., 2014; Yata et al., 2003). Since *Tbx18*-CreERT2 also produced robust labeling of sinoatrial node myocytes and venous myocardium (Figure S6A-D), atrial tissues were excluded from our analyses, which focused exclusively on the ventricular free walls and septum.

As expected, trichrome staining of histological sections revealed the existence of progressively increasing fibrosis in the left ventricular walls of TAC hearts, but not in sham operated controls (Figure 6B-D). *Col1a1*-GFP expression in sham hearts was typical of a

Author Manuscript Author Manuscript Author Manuscript Author Manuscript

healthy heart, with the transgene labeling fibroblasts and epicardial cells (Figure 6E), as previously reported (Moore-Morris et al., 2014). As the epicardial layer was also labeled by *Tbx18*-CreERT2, epicardial cells were readily identified as GFP/tdTomato double positive cells (arrows in Figure 6E-G). The amount of *Col1a1*-GFP^{high} fibroblasts was dramatically increased in TAC hearts (Figure 6F-G). Interestingly, even though trichrome stainings revealed stronger fibrosis at 28d post-TAC, the most significant expansion of the *Col1a1*-GFP^{high} fibroblast population was detected at 7d post-TAC. Such differences reflect the distinct specificities of both stainings: *Col1a1*-GFP detects cells actively producing Collagen, whereas trichrome allows for visualization of extracellular Collagen fibers deposited over time.

Importantly, apart from the double-labeled epicardium, we did not find evidence for significant overlap between *Col1a1*-GFP^{high} fibroblasts and tdTomato+ lineage traced cells at any of the TAC timepoints, indicating that pericytes were not major cellular precursors of fibrotic fibroblasts (Figure 6E-G). Interestingly, however, activation of low levels of *Col1a1*-GFP expression was observed in a small subset of tdTomato+ lineage-traced cells following TAC. However, these cells retained expression of the pericyte/vascular smooth cell marker CD146, demonstrating they had maintained a mural cell identity. Such observations suggested that a subset of pericytes/vascular smooth muscle cells might contribute to fibrosis by adopting an “activated” state in response to injury, but that they were not the cellular progenitors of fibrotic fibroblasts responsible for the majority of collagen production. Immunostaining of cryosections from sham and TAC hearts with an antibody recognizing the myocyte marker α-sarcomeric actinin revealed that pericytes did not significantly contribute to cardiomyocytes post-TAC. No *Tbx18*-CreERT2 lineage-traced cardiomyocytes were observed at 1-week post-TAC (n=3, 20 histological sections per heart, Figure 6H). At 4-weeks post-TAC, two out of three hearts analyzed displayed extremely rare examples of lineage-traced ventricular cardiomyocytes (1 cardiomyocyte in one heart and 2 in the second, 20 histological sections per heart, Figure S6E-F), likely resulting from cardiomyocyte-pericyte fusion events (Alvarez-Dolado et al., 2003). Lack of pericyte-to-myocyte transdifferentiation is in agreement with previous work reporting pre-existing myocytes as the source of new myocytes in aging or post myocardial injury (Senyo etal., 2013).

Previous studies have suggested that pericytes can act as myogenic progenitors in skeletal muscle (Dellavalle et al., 2011; Dellavalle et al., 2007). Given the absence of myogenic potential of cardiac pericytes, we tested the myogenic potential of adult skeletal muscle pericytes in an injury setting. *Tbxl8$^{ERT2Cre/Wt}$;Rosa26$^{dToma/Wt}$;Collal*-GFP+ animals were induced as described above, and subsequently subjected to a single intra-tibialis anterioris injection of 10 μL of a 1.2% barium chloride (BaCl) solution. Compared to non-injected animals (Figure 6I), injured muscles displayed, one-day post BaCl injection, myofiber disorganization indicative of myocyte death (Figure 6J). 3-days post-injury, dead myofibers were replaced by an extensive scar, composed mainly of *Collal*-GFP^{high} fibroblasts and CD45+ immune cells (Figure 6K). 7-days post-injury most of the fibrotic scar was resolved, and replaced by new skeletal myocytes (Figure 6L). Importantly, *Tbxl8*-CreERT2*;tdTomato* expression did not co-localize with either *Collal*-GFP^{high} fibroblasts or skeletal myocytes

Author Manuscript Author Manuscript Author Manuscript Author Manuscript

indicating that pericytes/vascular smooth muscle cells did not contribute to either of these two populations in this injury setting.

Brain pericytes are not progenitors of neurons or scar tissue

Central nervous system pericytes have been proposed to function as the major contributor to fibrotic scarring (Goritz et al., 2011), as progenitors of microglia (Sakuma et al., 2016), and as progenitors of neurons, astrocytes and oligodendrocytes (Dore-Duffy et al., 2006; Nakagomi et al., 2015). However, our studies revealed that brain pericytes maintained their identity and did not transdifferentiate into other lineages during aging (Figure 4). To test the plasticity of brain pericytes and vascular smooth muscle cells in a pathological setting, we followed the fate of *Tbx18*-CreERT2 lineage traced cells in response to cortical stab wounds. As expected (Silver and Miller, 2004), in response to injury, the brain produced a glial scar mainly composed of reactive astrocytes and macrophages/microglial cells (Figure 7A). Importantly, out of 9 animals analyzed (3 per time point after injury, 20 sections per animal), *Tbx18*-CreERT2 lineage traced cells did not co-localize with markers of astrocytes (GFAP, Figure 7A), macrophages/microglia (CD45, Figure 7A), or neurons (TrKB, Figure 7B), and retained expression of the pericyte/vascular smooth muscle cell marker PDGFRβ (Figure 7B), indicating they maintained their identity and did not function as stem cells in this injury setting. Consistent with this lack of stemness, we did not observe any expansion of the *Tbx18*-CreERT2 lineage traced population post-injury (Figure 7). To look at fibrotic responses, we performed a similar injury on mice that also harbored the *Col1a1*-GFP transgene (Yata et al., 2003). In non-injured cortical tissue, *Col1a1*-GFP signal was detected in subsets of *Tbx18*-CreERT2 lineage traced cells: pia mater and mural cells of larger vessels (Figure 7C). Although, no substantial increase in Collagen expressing cells was observed following injury, a small number of *Col1a1*-GFP+ fibroblasts were detected at the tip of the wound, 4 days post-surgery (Figure 7C). Notably, these fibroblasts were not *Tbx18*-CreERT2; tdTomato lineage-labeled and thus were not derived from pericytes or vascular smooth muscle.

TBX18 does not limit plasticity of mural cells

Our observation that cultured mural cells expressed lower levels of *Tbx18* than their in vivo counterparts raised the possibility that lack of mural cell plasticity in vivo versus the multi-lineage potential observed in vitro could be a result of transcriptional expression programs regulated by TBX18. To test this possibility, we generated a floxed *Tbx18* allele in which exon 2, encoding a critical DNA binding domain, could be conditionally ablated (Figure S7A). *Tbx18* homozygous floxed animals developed normally and had a normal lifespan. Animals homozygous for the floxed-out (null) *Tbx18* allele displayed the same phenotypic manifestations as germline *Tbx18* KOs (Bussen et al., 2004), and died cyanotic shortly after birth, validating this floxed allele as an effective line for conditional depletion of TBX18.

Tamoxifen administration to 8-week-old $Tbx18^{ERT2Cre/flox};Rosa26^{tdToma/Wt}$ animals and consequent deletion of TBX18 in *Tbx18*-expressing lineages did not limit animal viability, or increase plasticity of mural cells during aging (data not shown). Challenging $Tbx18^{ERT2Cre/flox};Rosa26^{tdToma/Wt}$ animals (skeletal muscle injury models and high-fat diet) produced results comparable to those observed in $Tbx18^{ERT2Cre/WT};Rosa26^{tdToma/Wt}$

Author Manuscript Author Manuscript Author Manuscript Author Manuscript

controls. That is, that no appreciable labeling of skeletal muscle fibers (0 labeled myocytes out of 4 animals per genotype, 32 sections per animal, Figure S7C) was observed in injured skeletal muscle, and rates of adipocyte labeling in animals on a high fat diet were comparable to those observed at time zero (less than 0.01% of adipocytes labeled, 3 animals per genotype, 20 sections per animal, Figure S7B). Together, these results demonstrated that TBX18 function did not pose a barrier to potential MSC behavior of pericytes in vivo, and that MSC behavior of pericytes in vitro was unlikely to be a result of reduced TBX18 expression.

Discussion

In a restricted number of organs, existence of dedicated pools of stem cells occupying specific niches has been extensively characterized (Fuchs et al., 2004). These progenitors ensure tissue homeostasis by replenishing aged or damaged cells and, under pathological circumstances, can generate new cellular units for tissue repair. The discovery that, in vitro, pericytes display multi-lineage potential suggested that endogenous pericytes might contribute to tissue repair and regeneration by replacing different cell types lost consequent to injury, and that this regenerative potential might be harnessed to further promote tissue healing (a particularly attractive prospect considering the ubiquitous distribution of pericytes). However, most observations placing pericytes as tissue-resident progenitors have been inferred following isolation and in vitro culture of pericytes.

Although the biology of pericytes has been extensively studied by multiple groups (Armulik et al., 2011), few specific tools have been available to address the potential cell fates of pericytes in vivo either during aging or in injury settings. As demonstrated in Figure 3, the constitutive *Pdgfrb*-Cre is unsuitable for pericyte lineage tracing and this observation is likely valid for other constitutively expressed recombinases, as markers of pericytes in adulthood are typically broadly expressed during embryogenesis.

Here we describe two alleles, *Tbx18*-H2B:GFP and *Tbx18*-CreERT2 as being selectively expressed by pericytes and vascular smooth muscle in multiple adult organs. *Tbx18* reporter expression was not observed in all organs analyzed. However, in tissues that did display pericyte/vascular smooth muscle cell expression of *Tbx18*, expression was not confined to a subset of these cell types, but rather observed in all pericytes and vascular smooth muscle cells (Figure 2 C and D).

The *Tbx18*-CreERT2 allele reported here allows for accurate fate-mapping of pericytes and, when used in combination with a floxed allele, allows for generation of mural cell restricted conditional knockouts, facilitating in vivo studies of pericyte/vascular smooth muscle cell biology. Using this allele, we studied progeny of pericytes/vascular smooth muscle cells in brain, heart, tibialis anterioris skeletal muscle, and multiple fat depots in aging and pathological models. Contrary to in vitro results, our fate-mapping experiments revealed that in vivo pericytes retain their identity and do not differentiate into other cellular lineages. We found no evidence for pericyte-derived adipogenesis or myogenesis in aging or disease. In cardiac and skeletal muscle fibrosis, pericytes may make an incremental contribution to scar

Author Manuscript Author Manuscript Author Manuscript Author Manuscript

formation, not as progenitors of fibroblasts, but by transient acquisition of an activated phenotype characterized by expression of low-levels of *Collagen1a1*.

In summary, our results suggest that endogenous adult pericytes of heart, brain, skeletal muscle, and fat depots do not behave as multipotent tissue-resident progenitors and suggest that plasticity observed in vitro or following transplantation in vivo might be consequent to the artificial cell culture environment. In this regard, it is important to note that a large number of studies that have suggested that pericytes behave as MSCs have focused on pericytes from the tissues we have examined here (Chen et al., 2015; Crisan et al., 2008; Dellavalle et al., 2011; Dellavalle et al., 2007; Dore-Duffy et al., 2006; Paul et al., 2012; Tang et al., 2008). Similar in vitro versus in vivo discrepancies in progenitor potential have been recently observed for cardiac c-Kit+ cells (van Berlo et al., 2014), highlighting the importance of lineage tracing studies for the study of progenitors in their endogenous niche (Snippert and Clevers, 2011). Although our observations discourage the use of pericytes within the relevant tissues as endogenous progenitors for regeneration, they do not challenge the beneficial effects of injecting previously cultured pericytes into injured organs. However, further studies will be necessary to determine whether cultured pericytes present any advantage when compared to injection of pre-differentiated patient-specific iPS cells. Results presented here apply exclusively to bona fide pericytes and vascular smooth muscle and do not exclude that other cell lineages located within or in the vicinity of the vascular niche might act as tissue-resident progenitors. Similarly, our results also do not exclude that pericytes of organs other than the ones explored here might display plasticity in vivo.

Contact for Reagent and Resource Sharing

Requests for reagent and resource sharing should be addressed to the corresponding author: Sylvia M. Evans, University of California, San Diego, syevans@ucsd.edu.

Experimental Model and Subject Details

Mice

All animal care was in compliance with the *Guide for the Care and Use of Laboratory Animals* published by the US National Institutes of Health, as well as institutional guidelines at the University of California, San Diego. All transgenic lines used were kept on an outbred background (Black-Swiss, Charles River laboratories). Mice were maintained in disposable plastic cages with filtered air intake ports (Innovive Inc) on a 12-hour light cycle and fed Teklad LM-485 irradiated diet (Harlan Laboratories, catalog number 7912). All analyses were performed on a minimum of 3 animals per time point. For analyses conducted in embryonic stages, embryos were staged according to the embryonic day (E) on which dissection took place, with noon of the vaginal plug day being considered as E0.5 and birth typically occurring at E19.

Pdgfrb-Cre, expressing Cre recombinase under the control of a fragment of the *Pdgfrb* promotor (Foo et al., 2006) was a kind gift from Ralf Adams. *Tie2*-Cre, expressing Cre recombinase under the control of the *Tie2* promotor/enhancer (Kisanuki et al., 2001) was a king gift from Masashi Yanagisawa. The fibroblast marker *Collagen1a1*-GFP (Yata et al.,

Author Manuscript Author Manuscript Author Manuscript Author Manuscript

2003) was a kind gift of David Brenner. The *Rosa26:tdTomato* reporter allele generated by Hongkui Zeng (Madisen et al., 2010) was obtained from the JAX laboratories (stock number 007905). The *Tbx18*-H2B:GFP transcriptional indicator was generated in our laboratory and has been previously shown to faithfully recapitulate the patterns of *Tbx18* expression inferred using RNA *in situ* (Cai et al., 2008). The *Tbx18*-CreERT2 allele was generated by knocking a CreERT2_FRT_PGK-Neo_FRT cassette into the *Tbx18* locus, 6 basepairs downstream of the endogenous ATG. Successfully targeted embryonic stem cells were identified by Southern blot and injected into blastocysts to produce chimeric mice. Confirmation of germline transmission of the targeted allele allowed for the propagation of the *Tbx18*-CreERT2 line. Prior to the expansion of this line, animals were crossed with FLPase mice (Raymond and Soriano, 2007) to remove the FRT-flanked selection cassette and, this way, avoid potential interferences on gene expression caused by the presence of this exogenous DNA fragment. To generate a floxed *Tbx18* allele, loxP sites were inserted flanking both extremes of exon 2 of the endogenous *Tbx18* gene, encoding part of the DNA-binding domain critical for TBX18 activity.

Induction of recombinase activity in $Tbx18^{ERT2Cre/Wt};Rosa26^{tdToma/Wt}$ animals was achieved by intra-peritoneal injection of a 10 mg/mL tamoxifen solution. Tamoxifen was purchased from Sigma (catalog number T5648), dissolved in 10 mL of 100% ethanol and subsequently diluted in 90 mL of sesame oil (Sigma, catalog number S3547). Aliquots were stored at -20°C for a maximum of 6 months.

For adipogenesis experiments, tamoxifen-induced $Tbx18^{ERT2Cre/Wt};Rosa26^{tdToma/Wt}$ animals were transferred to a Teklad high fat diet with 1.25% cholesterol and 21% milkfat (Envigo, catalog number 96121) for 6 weeks. At the end of the 6-week treatment, relative increase in body weight in high-fat diet fed animals and lean chow fed controls was determined as follows: (Final body weight – Initial body weight)/Initial body weight × 100. For induction of cardiac fibrosis, animals were subjected to trans-aortic constriction as previously described (Rockman et al., 1991) and sacrificed at 1 and 4 weeks post surgery. For induction of skeletal muscle injuries, animals were anesthetized with ketamine/xylazine and received a single injection of 10 μL of a 1.2% BaCl solution (prepared in sterile, molecular biology grade water) in the tibialis anterioris muscle. Animals were sacrificed at 1, 3 and 7 days post-injury. For cortical brain stab-wounds mice were anesthetized with inhaled isoflurane. After a medial incision to open the scalp, mice were transferred to a stereotaxic device and physical disruption of cortical tissues induced by insertion (3 times) of a Hamilton syringe in the following coordinates: AP-2; ML+1.5; DV1.3.

Primary cultures of mural cells

Mural cells were isolated from $TBX18^{H2B:GFP/WT}$ animals and maintained in MSC growing medium (DMEM:F12; 20% FBS, 1% P/S), being passaged once a week. For details on isolation, culture and differentiation of primary mural cells, please see Method Details section.

Author Manuscript Author Manuscript Author Manuscript Author Manuscript

Method Details

Genotyping of Transgenic Animals

For genotyping of transgenic animals, tail biopsies were collected at weaning (3-week-old). Presence or absence of the *Collagenlal*-GFP transgene was directly detected by examination of the tail biopsy under a fluorescent microscope. All other alleles were detected by PCR using the primers described in Table S2.

Fluorescent immunohistochemistry/immunocytochemistry

Cultured cells were fixed in 4% paraformaldehyde (Electron Microscope Sciences) for 10 minutes at room temperature and stored at 4°C in PBS. Dissected retinas were fixed overnight in 4% paraformaldehyde at 4°C and stored, up to a week, at 4°C in PBS. All other dissected tissues were fixed overnight in 4% paraformaldehyde at 4°C, dehydrated in a sucrose gradient and frozen in O.C.T. compound (Tissue-Tek). Histological sections (50μm thick for white adipose depots and 10μm thick for all other tissues) were prepared from frozen blocks using a Leica CM3050S cryostat. Tissue sections, adherent cultured cells, or whole-mount retinas were permeabilized in PBS-0.1% Triton for 10 minutes and incubated for one hour at room temperature in blocking solution (PBS-0.1% Triton, 10% donkey serum, 5% skim milk) prior to overnight primary antibody incubation (4°C). A list of all primary antibodies used, their providers and dilutions can be found in the next page. AlexaFluor-conjugated secondary antibodies (Life Technologies) diluted 1:400 in blocking solution were used for detection of primary antibodies and DAPI (Life Technologies) used for labeling of nuclei. Image acquisition was performed using an Olympus FVI000 confocal microscope and image editing done using the Olympus software Fluoview or ImageJ. Thrichrome staining of tissue sections was performed using the Masson thrichrome stain kit (Sigma, HT15), following instructions provided by the manufacturer. Staining of lipid droplets in tissue sections was achieved using the Oil Red O stain kit (Diagnostic BioSystems, KT 025-IFU), following instructions provided by the manufacturer.

FACS analyses

For flow cytometry analyses of bone marrow populations, cell preps were obtained by flushing tibias and femurs with 5 mL ice cold PBS. Masses of bone marrow were transferred into sterile 10cm plastic dishes and physically dissociated into a single cell suspension by performing 10 cycles of aspiration and ejection against the bottom of the plastic dish, using a 10mL syringe without needle. Cellular suspensions were then filtered through a 40 μn cell strainer. After centrifugation at 300g, 4°C, for 10 minutes, the supernatant was discarded and cells ressuspended in 500 μL of FACS buffer (HBSS without calcium or magnesium, supplemented with 5% FBS). Immediately prior to analysis in a BD FACS Canto, 1 μL of DAPI was added to allow gating of dead cells. To allow gating of tdTomato- and tdTomato+ populations, isolations were done in Cre- and Cre+ (*Tie2*-Cre or *Pdgfrb*-Cre) animals. Post-acquisition analyses and processing of FACS data were performed using FlowJo.

Author Manuscript Author Manuscript Author Manuscript Author Manuscript

Isolation, in vitro propagation and differentiation of *Tbxl8*-GFP+ mural cells

Initial experiments to determine whether Tbxl8+ mural cells are endowed with progenitor potential were carried in vitro, using purified populations of Tbxl8GFP+ cells. To this end, two-month old $Tbx18^{GFP/WT}$animals were sacrificed by cervical dislocation and thoroughly sprayed with 70% ethanol. Peri-gonadal fat depots were dissected and minced into small pieces with sterile scissors. Tissues were then enzymatically digested in a sterile HBSS solution (Corning Cellgro, 21-023-CV) containing 10 mg/mL collagenase/dispase (Roche, 269638), 200U/mL DNase I (Sigma, D4513), 1% (V/V) P/S (Gibco, 15140-122) and 1% (V/V) Fungizone (Gibco, 15290-018) for one hour at 37°C, under permanent agitation. Clumps of undigested tissue were removed by filtering through a 40 μn cell strainer. Centrifugation at 300g, 4°C, for 10 minutes allowed for individualization of two clear cell fractions: a Stromal Vascular Fraction (SVF) pelleted in the bottom of the tube and a layer of adipocytes fluctuating in the supernatant. The later were discarded and the SVF ressuspended in 200 μL of FACS buffer (HBSS supplemented with 5% FBS) and stained for 30 minutes at 4°C with PE-CD146 and APC-CD31 antibodies. After three 5-minute washes in FACS buffer, cells were ressupended in 500 μL of FACS buffer supplemented with 1 μL of DAPI (used for identification of dead cells). Cellular suspensions were immediately run on a BD FACSAria III and DAPI-; CD146+; CD31-; GFP+ mural cells sorted into adhesion-inducing medium (DMEM:F12 - Gibco, 10565-018; 50% FBS - Gibco, 16000-044; 1% P/S and 1% Fungizone). Sorted cells were seeded in 6-well tissue culture plates, at a density of 6×10^4 cells/well. 24 hour post platting, cultured cells were transferred to standard MSC growing medium (DMEM:F12; 20% FBS, 1% P/S) supplemented with 1% Fungizone. Fungizone was withdrawn from culture medium after the first week of culture and cells were grown in this medium for seven days. From this point onwards, cells were propagated according to standard cell culture methods, being weekly passaged at a ratio of 1:3.

Capacity to differentiate into distinct cellular lineages was assessed by culture in media formulated to drive acquisition of specific cell fates. Briefly, cells from passages 5 to 15 were plated in 6-well plates (10^5 cells/well) and expanded in MSC growing medium until reaching 80%) confluency. At this point, cells were incubated in one of the following media, for the specified time:

- Induction of osteoblastic differentiation: cells cultured for 21 days in DMEM, 5% FBS, 100 nM dexamethasone (Sigma-Aldrich, D4902), 50 μM L-ascorbic acid-2-phosphate (Sigma-Aldrich, 49752), 10 mM β-glycerophosphate (Sigma-Aldrich, G9422), 300 ng/mL BMP2 (Cell Signaling, 4697) and 1% P/S. After 21 days of treatment with differentiation medium, cultures were fixed in 4% PFA for ten minutes and stained for ten minutes with a 2% Alizarin red S solution, pH 4.2 (Sigma-Aldrich, A5533) to identify deposition of mineralized matrix, indicative of osteoblastic differentiation.
- Induction of adipogenic differentiation: cells were cultured for 3 days in DMEM:F12, 10% FBS, 500 μM IBMX (l-methyl-3 isobutylxanthine, Sigma-Aldrich, 17018), 1 μM dexamethasone (Sigma-Aldrich, D4902), 200 μM indomethacin (Sigma-Aldrich, 18280), 1% Insulin-Transferrin-Selenium-X (Gibco, 51500) and 1% P/S. After 3 days of adipogenic induction, cells were

Author Manuscript Author Manuscript Author Manuscript Author Manuscript

cultured for 4 to 7 days in regular MSC growing medium supplemented with 1% Insulin-Transferrin-Selenium-X (Gibco, 51500). Cultures were then fixed in 4% PFA for ten minutes and stained, for five minutes, with Oil Red O to identify lipid vacuoles. Oil Red O working solution = l.0g of Oil Red O powder (Sigma-Aldrich, O0625) dissolved in 50 mL of a 1:1 solution of 70% ethanol and acetone.

- Induction of chondrogenic differentiation was based on a high-density (micromass) culture. 10 μL of a suspension of cultured mural cells at a density of 10^6 cells/mL were plated in the center of the wells of a 12-well culture plate. Cells were allowed to attach for 3 to 4 hours and 1 mL of chondrogenic medium was added to each well. Chondrogenic medium = DMEM:F12, 1% FBS, 1% Insulin-Transferrin-Selenium-X (Gibco, 51500), 50μg/mL L-ascorbic acid-2-phosphate (Sigma-Aldrich, 49752), 10.0ng/mL TGFβ1 (Peprotech, 100-21), and 1% P/S. Cells were then cultured for 10 to 14 days in chondrogenic medium with careful handling to avoid dislodgment of cellular pellets. For confirmation of differentiation into cartilage, micromass cultures were fixed in 4% PFA for ten minutes and stained with alcian blue for 30 minutes. Alcian blue working solution = 1% alcian blue 8GX solution (Sigma-Aldrich, 66011) prepared in 0.1N HCl, pH 1.0.

Immuno-gold Electron Microscopy

For immunoelectron microscopic studies, *Tbx18*$^{GFP/WT}$ animals and *Tbx18*$^{WT/WT}$ negative controls were anesthetized with ketamine/xylazine and perfused, through the left ventricle of the heart, with 5 mL PBS and 5 mL of 4% PFA in 0.1 M phosphate buffer. Brains were dissected and cortical tissues were then cut into small cubes (approximately 1 × 1 × 1mm), fixed for 12h in 4% PFA in 0.1 M phosphate buffer, pelleted in 10% gelatin, cryoprotected in sucrose, and snap frozen in liquid nitrogen. Immunogold labeling of nuclear GFP was achieved by incubation of ultrathin cryosections (70–80 nm) with a mouse anti-GFP IgG (2 hours, Clontech, 632381), followed by incubation, for one hour, with goat anti-mouse IgG-gold conjugates. Immuno-gold stained sections were then contrasted for 10 minutes in 0.4% uranyl acetate and 1.8% methylcellulose on ice. Imaging was carried out at the Cellular and Molecular Medicine Electron Microscopy Facility (University of California, San Diego), using a JEOL 1200 EX II electron microscope equipped with an Orius CCD Gatan camera and Gatan digital micrograph software.

Quantification and Statistical Analysis

All labeling quantifications were performed in 3 animals, with a minimal of 50 cells being counted per animal. In all graphs, data are presented as mean ± standard deviation.

Data and Software Availability

A complete list of software for data analysis and processing can be found in the Key Resources Table.

Author Manuscript Author Manuscript Author Manuscript Author Manuscript

Supplementary Material

Refer to Web version on PubMed Central for supplementary material.

Acknowledgments

NGC received a doctoral fellowship (SFRH/BD/32983/2006) from the Portuguese Foundation for Science and Technology. PC was supported by a Marie Curie International Outgoing Fellowship (PIOF-623739). YFS was supported by grants from the Ministry of Science and Technology China (2013CB967400) and National Natural Science Foundation of China (NSFC) (81570285). This work was supported by NIH grants to JC and SME. JC is American Heart Association Endowed Chair in Cardiovascular Research. Imaging was performed at the UCSD Neuroscience Microscopy Facility supported by the NIH grant P30 NS047101. Authors thank Jennifer Santini for microscopy assistance, Timo Meerloo and Vanessa Taupin for assistance with immuno-EM techniques, and Dieu Hung Lao for help with the skeletal muscle injury model. *Pdgfrb*-Cre was a kind gift from Ralf H. Adams.

References

Alvarez-Dolado M, Pardal R, Garcia-Verdugo JM, Fike JR, Lee HO, Pfeffer K, Lois C, Morrison SJ, Alvarez-Buylla A. Fusion of bone-marrow-derived cells with Purkinje neurons, cardiomyocytes and hepatocytes. Nature. 2003; 425:968–973. [PubMed: 14555960]

Armulik A, Genove G, Betsholtz C. Pericytes: developmental, physiological, and pathological perspectives, problems, and promises. Developmental cell. 2011; 21:193–215. [PubMed: 21839917]

Ben-David U, Benvenisty N. The tumorigenicity of human embryonic and induced pluripotent stem cells. Nature reviews Cancer. 2011; 11:268–277. [PubMed: 21390058]

Bohnenpoll T, Bettenhausen E, Weiss AC, Foik AB, Trowe MO, Blank P, Airik R, Kispert A. Tbx18 expression demarcates multipotent precursor populations in the developing urogenital system but is exclusively required within the ureteric mesenchymal lineage to suppress a renal stromal fate. Dev Biol. 2013; 380:25–36. [PubMed: 23685333]

Buckingham ME, Meilhac SM. Tracing cells for tracking cell lineage and clonal behavior. Developmental cell. 2011; 21:394–409. [PubMed: 21920310]

Bussen M, Petry M, Schuster-Gossler K, Leitges M, Gossler A, Kispert A. The T-box transcription factor Tbx18 maintains the separation of anterior and posterior somite compartments. Genes Dev. 2004; 18:1209–1221. [PubMed: 15155583]

Cai CL, Martin JC, Sun Y, Cui L, Wang L, Ouyang K, Yang L, Bu L, Liang X, Zhang X, et al. A myocardial lineage derives from Tbx18 epicardial cells. Nature. 2008; 454:104–108. [PubMed: 18480752]

Chen WC, Baily JE, Corselli M, Diaz ME, Sun B, Xiang G, Gray GA, Huard J, Peault B. Human myocardial pericytes: multipotent mesodermal precursors exhibiting cardiac specificity. Stem Cells. 2015; 33:557–573. [PubMed: 25336400]

Crisan M, Yap S, Casteilla L, Chen CW, Corselli M, Park TS, Andriolo G, Sun B, Zheng B, Zhang L, et al. A perivascular origin for mesenchymal stem cells in multiple human organs. Cell stem cell. 2008; 3:301–313. [PubMed: 18786417]

Dellavalle A, Maroli G, Covarello D, Azzoni E, Innocenzi A, Perani L, Antonini S, Sambasivan R, Brunelli S, Tajbakhsh S, et al. Pericytes resident in postnatal skeletal muscle differentiate into muscle fibres and generate satellite cells. Nat Commun. 2011; 2:499. [PubMed: 21988915]

Dellavalle A, Sampaolesi M, Tonlorenzi R, Tagliafico E, Sacchetti B, Perani L, Innocenzi A, Galvez BG, Messina G, Morosetti R, et al. Pericytes of human skeletal muscle are myogenic precursors distinct from satellite cells. Nature cell biology. 2007; 9:255–267. [PubMed: 17293855]

Dore-Duffy P, Katychev A, Wang X, Van Buren E. CNS microvascular pericytes exhibit multipotential stem cell activity. J Cereb Blood Flow Metab. 2006; 26:613–624. [PubMed: 16421511]

Foo SS, Turner CJ, Adams S, Compagni A, Aubyn D, Kogata N, Lindblom P, Shani M, Zicha D, Adams RH. Ephrin-B2 controls cell motility and adhesion during blood-vessel-wall assembly. Cell. 2006; 124:161–173. [PubMed: 16413489]

Fuchs E, Tumbar T, Guasch G. Socializing with the neighbors: stem cells and their niche. Cell. 2004; 116:769–778. [PubMed: 15035980]

Author Manuscript Author Manuscript Author Manuscript Author Manuscript

Goritz C, Dias DO, Tomilin N, Barbacid M, Shupliakov O, Frisen J. A pericyte origin of spinal cord scar tissue. Science. 2011; 333:238–242. [PubMed: 21737741]

Greenhalgh SN, Iredale JP, Henderson NC. Origins of fibrosis: pericytes take centre stage. F1000prime reports. 2013; 5:37. [PubMed: 24049641]

Kapoor N, Liang W, Marban E, Cho HC. Direct conversion of quiescent cardiomyocytes to pacemaker cells by expression of Tbx18. Nature biotechnology. 2013; 31:54–62.

Kisanuki YY, Hammer RE, Miyazaki J, Williams SC, Richardson JA, Yanagisawa M. Tie2-Cre transgenic mice: a new model for endothelial cell-lineage analysis in vivo. Dev Biol. 2001; 230:230–242. [PubMed: 11161575]

Kraus F, Haenig B, Kispert A. Cloning and expression analysis of the mouse T-box gene Tbx18. Mechanisms of development. 2001; 100:83–86. [PubMed: 11118889]

Krautler NJ, Kana V, Kranich J, Tian Y, Perera D, Lemm D, Schwarz P, Armulik A, Browning JL, Tallquist M, et al. Follicular dendritic cells emerge from ubiquitous perivascular precursors. Cell. 2012; 150:194–206. [PubMed: 22770220]

Long JZ, Svensson KJ, Tsai L, Zeng X, Roh HC, Kong X, Rao RR, Lou J, Lokurkar I, Baur W, et al. A smooth muscle-like origin for beige adipocytes. Cell Metab. 2014; 19:810–820. [PubMed: 24709624]

Madisen L, Zwingman TA, Sunkin SM, Oh SW, Zariwala HA, Gu H, Ng LL, Palmiter RD, Hawrylycz MJ, Jones AR, et al. A robust and high-throughput Cre reporting and characterization system for the whole mouse brain. Nature neuroscience. 2010; 13:133–140. [PubMed: 20023653]

Moore-Morris T, Guimaraes-Camboa N, Banerjee I, Zambon AC, Kisseleva T, Velayoudon A, Stallcup WB, Gu Y, Dalton ND, Cedenilla M, et al. Resident fibroblast lineages mediate pressure overload-induced cardiac fibrosis. The Journal of clinical investigation. 2014; 124:2921–2934. [PubMed: 24937432]

Nakagomi T, Nakano-Doi A, Kawamura M, Matsuyama T. Do Vascular Pericytes Contribute to Neurovasculogenesis in the CNS as Multipotent Vascular Stem Cells? Stem cells and development. 2015

Paul G, Ozen I, Christophersen NS, Reinbothe T, Bengzon J, Visse E, Jansson K, Dannaeus K, Henriques-Oliveira C, Roybon L, et al. The adult human brain harbors multipotent perivascular mesenchymal stem cells. PloS one. 2012; 7:e35577. [PubMed: 22523602]

Raymond CS, Soriano P. High-efficiency FLP and PhiC31 site-specific recombination in mammalian cells. PloS one. 2007; 2:e162. [PubMed: 17225864]

Rockman HA, Ross RS, Harris AN, Knowlton KU, Steinhelper ME, Field LJ, Ross J Jr, Chien KR. Segregation of atrial-specific and inducible expression of an atrial natriuretic factor transgene in an in vivo murine model of cardiac hypertrophy. Proceedings of the National Academy of Sciences of the United States of America. 1991; 88:8277–8281. [PubMed: 1832775]

Sakuma R, Kawahara M, Nakano-Doi A, Takahashi A, Tanaka Y, Narita A, Kuwahara-Otani S, Hayakawa T, Yagi H, Matsuyama T, et al. Brain pericytes serve as microglia-generating multipotent vascular stem cells following ischemic stroke. J Neuroinflammation. 2016; 13:57. [PubMed: 26952098]

Sancho-Martinez I, Baek SH, Izpisua Belmonte JC. Lineage conversion methodologies meet the reprogramming toolbox. Nature cell biology. 2012; 14:892–899. [PubMed: 22945254]

Senyo SE, Steinhauser ML, Pizzimenti CL, Yang VK, Cai L, Wang M, Wu TD, Guerquin-Kern JL, Lechene CP, Lee RT. Mammalian heart renewal by preexisting cardiomyocytes. Nature. 2013; 493:433–436. [PubMed: 23222518]

Silver J, Miller JH. Regeneration beyond the glial scar. Nat Rev Neurosci. 2004; 5:146–156. [PubMed: 14735117]

Snippert HJ, Clevers H. Tracking adult stem cells. EMBO Rep. 2011; 12:113–122. [PubMed: 21252944]

Tang W, Zeve D, Suh JM, Bosnakovski D, Kyba M, Hammer RE, Tallquist MD, Graff JM. White fat progenitor cells reside in the adipose vasculature. Science. 2008; 322:583–586. [PubMed: 18801968]

Author Manuscript Author Manuscript Author Manuscript Author Manuscript

van Berlo JH, Kanisicak O, Maillet M, Vagnozzi RJ, Karch J, Lin SC, Middleton RC, Marban E, Molkentin JD. c-kit+ cells minimally contribute cardiomyocytes to the heart. Nature. 2014; 509:337–341. [PubMed: 24805242]

Wiese C, Grieskamp T, Airik R, Mommersteeg MT, Gardiwal A, de Gier-de Vries C, Schuster-Gossler K, Moorman AF, Kispert A, Christoffels VM. Formation of the sinus node head and differentiation of sinus node myocardium are independently regulated by Tbx18 and Tbx3. Circ Res. 2009; 104:388–397. [PubMed: 19096026]

Yata Y, Scanga A, Gillan A, Yang L, Reif S, Breindl M, Brenner DA, Rippe RA. DNase I-hypersensitive sites enhance alpha1(I) collagen gene expression in hepatic stellate cells. Hepatology. 2003; 37:267–276. [PubMed: 12540776]

Author Manuscript Author Manuscript Author Manuscript Author Manuscript

Highlights

- *Tbx18* is selectively expressed by pericytes in multiple adult organs
- A *Tbx18*-CreERT2 line allows for highly efficient labeling of pericytes in vivo
- In vivo, pericytes do not behave as stem cells during aging
- In vivo, pericytes do not behave as stem cells in pathological settings

Author Manuscript Author Manuscript Author Manuscript Author Manuscript

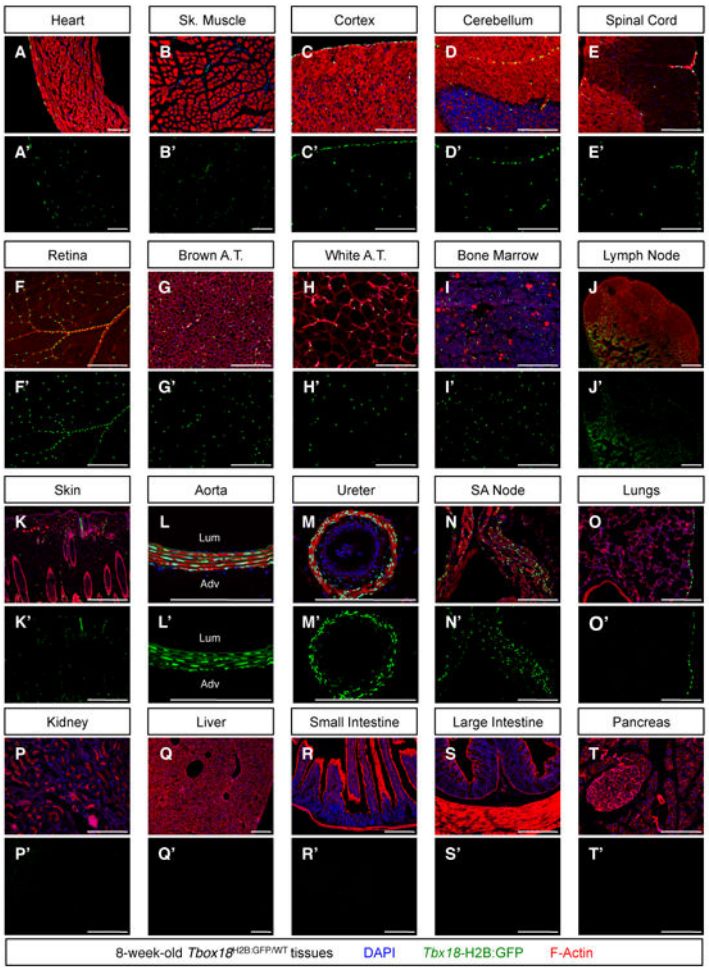


Figure 1. Patterns of *Tbxl8* expression in the adult mouse

To assess whether *Tbxl8* was actively expressed in adult tissues, organs were harvested from 8-week-old *Tbx18*$^{H2B:GFP/WT}$ mice and processed for histological analyses with the nuclear dye DAPI and with the filamentous actin marker Phalloidin. Confocal microscopy revealed strong H2B:GFP signal (indicative of active *Tbxl8* expression) in the membranous linings of: (**A**) the heart (epicardium), (**C-E**) the central nervous system (pia mater), and (**O**) the lungs (pleura). Expression by scattered interstitial cells was observed (**A**) within the cardiac ventricular walls, (**B**) in tibialis anterioris skeletal muscle, (**C-E**) in the central nervous system, (**F**) in the retina, (**G, H**) in interscapular brown and peri-gonadal white adipose depots, (**I**) in bone marrow, (**J**) in inguinal lymph nodes, and (**K**) in skin. Additionally, strong expression was observed (**L**) in the medial layer of the aorta, (**M**) in ureteric smooth muscle, and (**N**) in sinoatrial (SA) node pacemaker cells. No H2B:GFP signal could be detected (**P**) in the kidneys, nor (**Q-T**) the gastrointestinal tract or associated glands. Lum = lumen, Adv = adventitia. Bars = 200μm. See also Figure S1.

Author Manuscript Author Manuscript Author Manuscript Author Manuscript

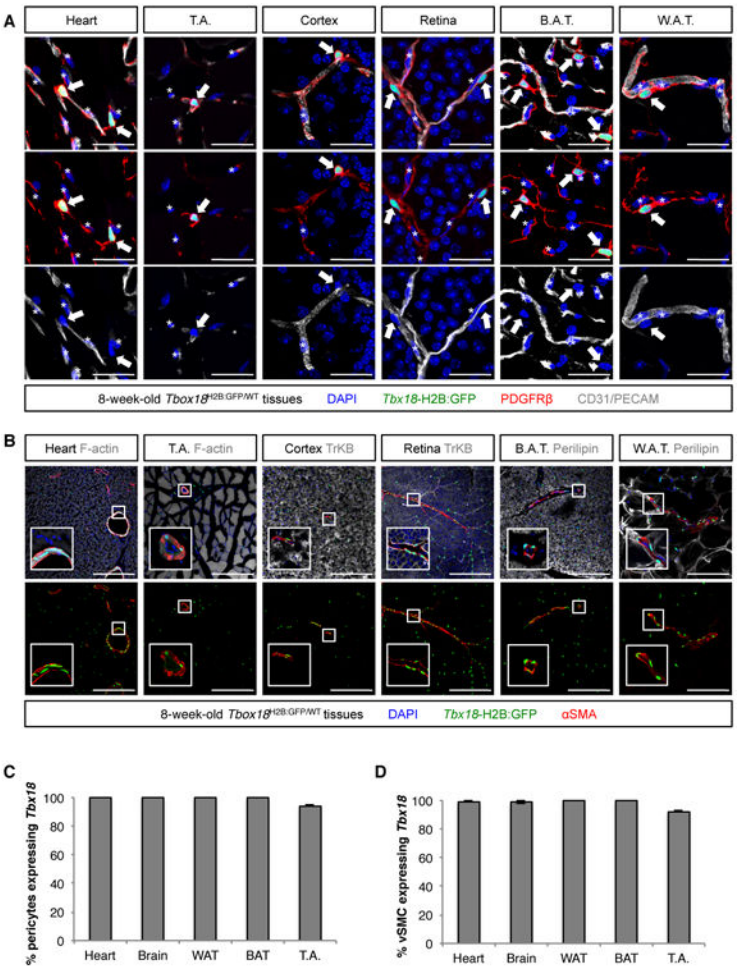


Figure 2. Interstitial *Tbxl8*-GFP+ cells were mural cells (pericytes and vascular smooth muscle)

(**A**) In all organs analyzed - heart, skeletal muscle of the tibialis anterioris (T.A.), cortex, retina, brown adipose tissue (B.A.T.) and white adipose tissue (W.A.T.) - interstitial *Tbxl8*-GFP+ cells (arrows) never expressed the endothelial marker CD31, but localized in the immediate vicinity of CD31+ endothelium and expressed the pan-pericyte marker PDGFRβ, emitting multiple cytoplasmic projections that enveloped adjacent blood vessels. Such location, morphology and cell-surface antigen profile placed interstitial *Tbxl8*-GFP+ cells as pericytes. Asterisks denote nuclei of endothelial cells. (**B**) In the vicinity of larger blood vessels, *Tbxl8*-GFP+ cells revealed a spindle shape and expressed the smooth muscle marker smooth muscle α actin (αSMA). (**C,D**) Importantly, in these organs, *Tbx18* expression did not mark a subset of mural cells, but rather the totality of pericytes (PDGFRβ, CD146 double positive cells) and vascular smooth muscle (αSMA+ cells). In C and D data are represented as mean ± standard deviation. Bars = 30μm in (A) and 200μm in (B). See also Figures S2 and S3, and Table S1.

Author Manuscript Author Manuscript Author Manuscript Author Manuscript

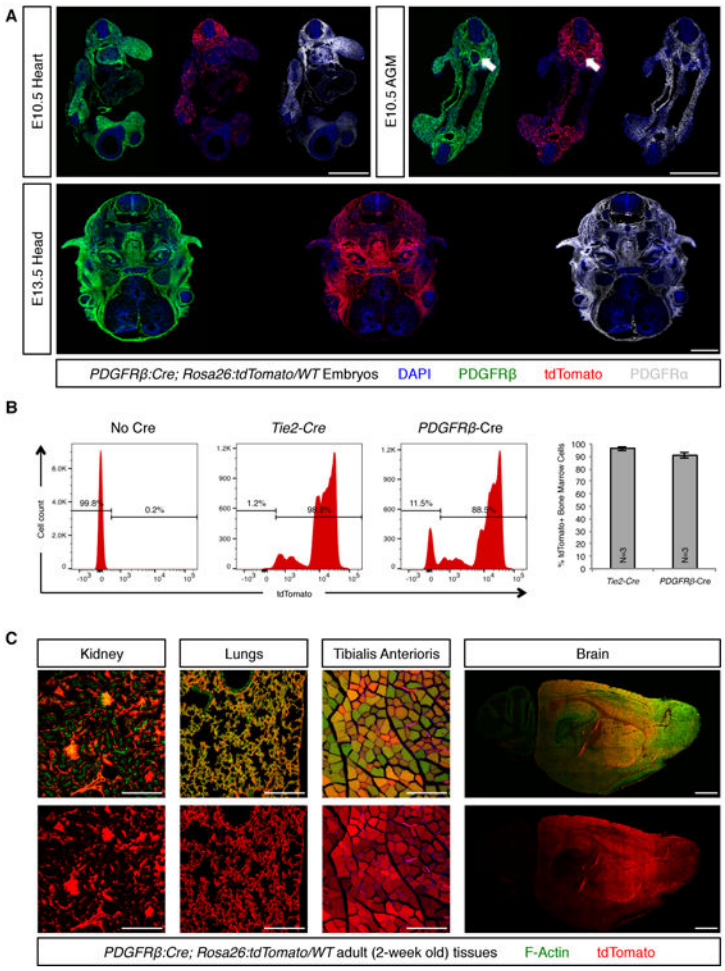


Figure 3. *Pdgfrb*-Cre was unsuitable for lineage tracing of pericytes

(A) PDGFRα (gray) and PDGFRβ (green) were expressed by multiple cell lineages during mid-gestational embryogenesis. Consequently, the constitutively active *Pdgfrb*-Cre extensively labeled multiple populations of embryonic progenitors (red channel), rendering it unsuitable for purposes of specific labeling of pericyte-derived lineages. Arrows indicate labeling of the aortic hemogenic endothelium by PDGFRβ and *Pdgfrb*-Cre in the aorta-gonad-mesonephros (AGM) region. (**B**) FACS analyses revealed that in adult animals *Pdgfrb*-Cre labeled the majority (approximately 90%) of all bone marrow cells, similar to the extent of labeling observed for the endothelial/hematopoietic *Tie2*-Cre. (**C**) Similarly, *Pdgfrb*-Cre labeled a majority of cells in multiple other tissues, including kidney, lungs, skeletal muscle and brain. Bars = 1000 μm in A and in brain montage, and 200 μm in all other panels. In B data are represented as mean ± standard deviation. See also Figure S4.

Author Manuscript Author Manuscript Author Manuscript Author Manuscript

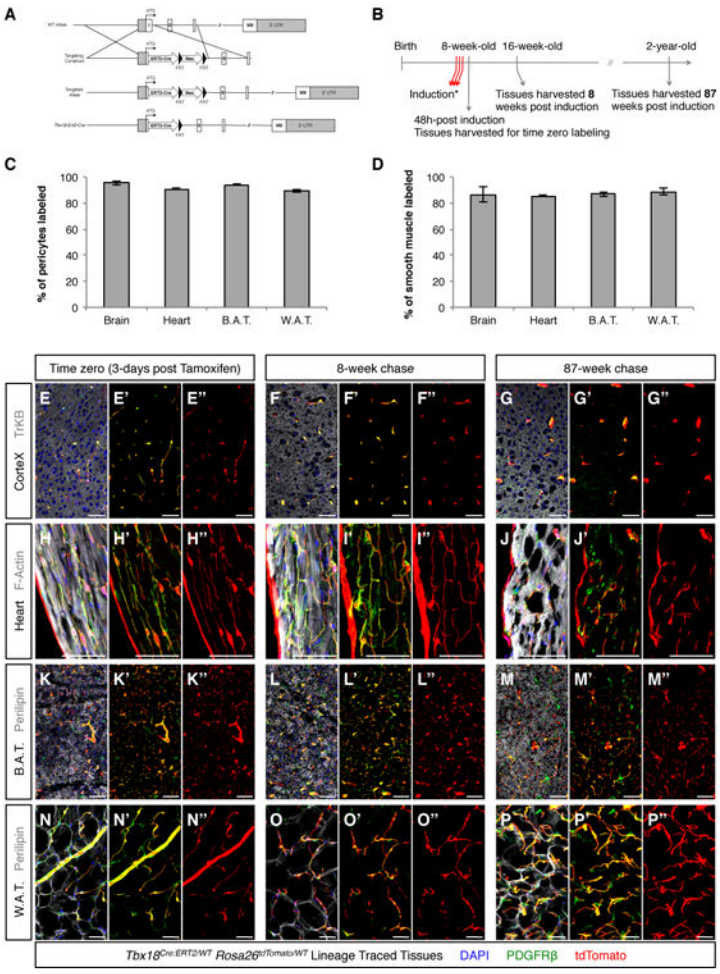


Figure 4. Pericytes and vascular smooth muscle cells maintained a mural cell phenotype during aging

(A) Strategy used to insert a CreERT2 cassette into the murine endogenous *Tbx18* locus. (**B**) Experimental design used for pulse-chase experiments aimed at determining the in vivo progenitor potential of pericytes during aging. **(C, D)** Intra-peritoneal administration of 1 mg of tamoxifen to adult (8-week-old) $Tbx18^{ERT2Cre/Wt};Rosa26^{tdTomato/Wt}$ animals for 3 consecutive days labeled more than 90% of pericytes and more than 85% of vascular smooth muscle in brain, heart, brown adipose tissue (B.A.T.) and white adipose tissue (W.A.T.). (**E-P**) Short (8-week) and long (87-week) aging experiments revealed that tdTomato+ lineage traced cells (red) in brain (**E-G**), heart (**H-J**), B.A.T. (**K-M**) and W.A.T. (**N-P**) never expressed tissue-specific parenchymal markers (gray), and always retained expression of the mural cell marker PDGFRβ (green), indicating pericytes and vascular smooth muscle cells had maintained their mural cell identity throughout aging. In C and D data are represented as mean ± standard deviation. Bars = 50μm. See also Figure S5.

Author Manuscript Author Manuscript Author Manuscript Author Manuscript

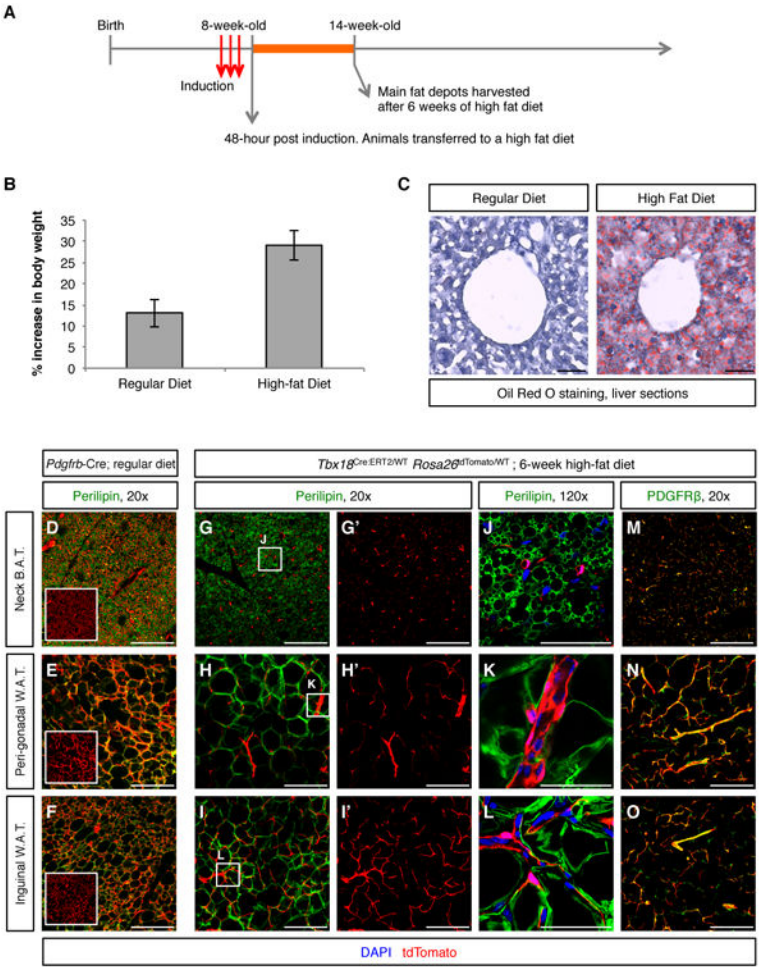


Figure 5. Mural cells were not adipogenic progenitors

(**A**) Experimental design for testing adipogenic potential of pericytes and vascular smooth muscle cells. (**B**) 6-week increase in body weight (expressed as percentage of starting weight) of animals fed a lean diet and animals fed a high-fat diet. (**C**) 6 weeks of high-fat diet resulted in hepatic steatosis. (**D-F**) *Pdgfrb*-Cre*;Rosa26*$^{tdTomato/Wt}$ lineage traced adipose depots isolated from regular diet fed animals were used as a positive control of adipocyte labeling by tdTomato. In these tissues, co-localization of the green (Perilipin) and red (tdTomato) signals produced an orange/yellow merge pattern. Boxed images are tdTomato-only panels to facilitate visualization of *Pdgfrb*-Cre-labeled cells. (**G-L**) In *Tbx18*$^{ERT2Cre/Wt}$*; Rosa26*$^{tdTomato/Wt}$ animals, even after 6 weeks of high fat diet, lineage traced cells did not co-localize with the adipocyte marker Perilipin in any of the fat depots analyzed. G′-I′ are the tdTomato-only panels of the images shown in G-I, respectively. J-L are higher magnification images of the areas boxed in G-I, respectively. (**M-O**) In addition to not showing expression of Perilipin, *Tbx18*-CreERT2-lineage traced cells retained expression of the mural cell marker PDGFRβ, demonstrating that pericytes and vascular smooth muscle cells had not functioned as progenitors of new adipocytes. Bars = 50μm in C, J, K, L and 200μm in all other panels. In B data are represented as mean ± standard deviation. See also Figure S7.

Author Manuscript Author Manuscript Author Manuscript Author Manuscript

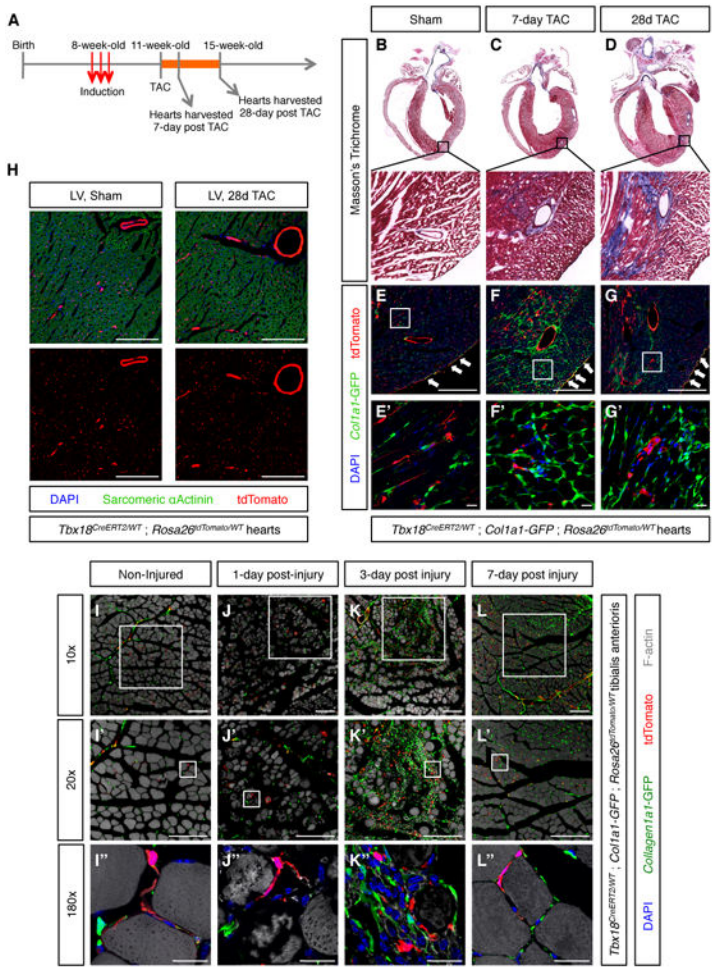


Figure 6. Pericytes were not progenitors of fibroblasts or myocytes

(A) Experimental design for testing whether cardiac pericytes were progenitors of fibroblasts or cardiomyocytes post-TAC. (**B-D**) Trichrome staining of histological sections demonstrated progressive accumulation of collagen fibers in TAC animals. Boxed areas are shown in higher magnification. (**E-G**) Confocal microscopy imaging of sections adjacent to those displayed in (B-D) revealed lack of co-localization between *Collal*-GFP^{high} fibroblasts and tdTomato+ pericytes and vascular smooth muscle in sham, but also TAC animals. E′-G′ are higher magnifications of areas boxed in E-G, respectively. (**H**) Confocal microscopy images showing absence of co-localization between tdTomato+ lineage traced cells and sarcomeric α-actinin+ cardiomyocytes. (**I-I′**) Non-injured tibialis anterioris muscle showing intact myofibers and non-overlapping populations of *Collal*-GFP^{high} fibroblasts and tdTomato+ *Tbxl8*-CreERT2 lineage-traced mural cells. (**J-J′**) 1 day post-injury, dying myofibers were observed in the vicinity of the BaCl injection site. (**K-K′**) 3 day post-injury, dead myofibers had been replaced by an extensive scar composed of *Collal*-GFP^{high} fibroblasts immune cells. Of note, the vast majority of *Collal*-GFP^{high} fibroblasts were not lineage traced by *Tbxl8*-CreERT2, revealing they were not derived from pericytes or vascular smooth muscle. (**L-L′**) 7 days post-injury, most of the scar tissue had been replaced by new myofibers. Newly formed myofibers were not lineage-traced by *Tbxl8*-CreERT2,

Author Manuscript Author Manuscript Author Manuscript Author Manuscript

demonstrating that pericytes and vascular smooth muscle had not functioned as progenitors of new myocytes. Bars = 20μm in (E′-G′), (I″-L″), and 200μm in all other panels. See also Figures S6 and S7.

Author Manuscript Author Manuscript Author Manuscript Author Manuscript

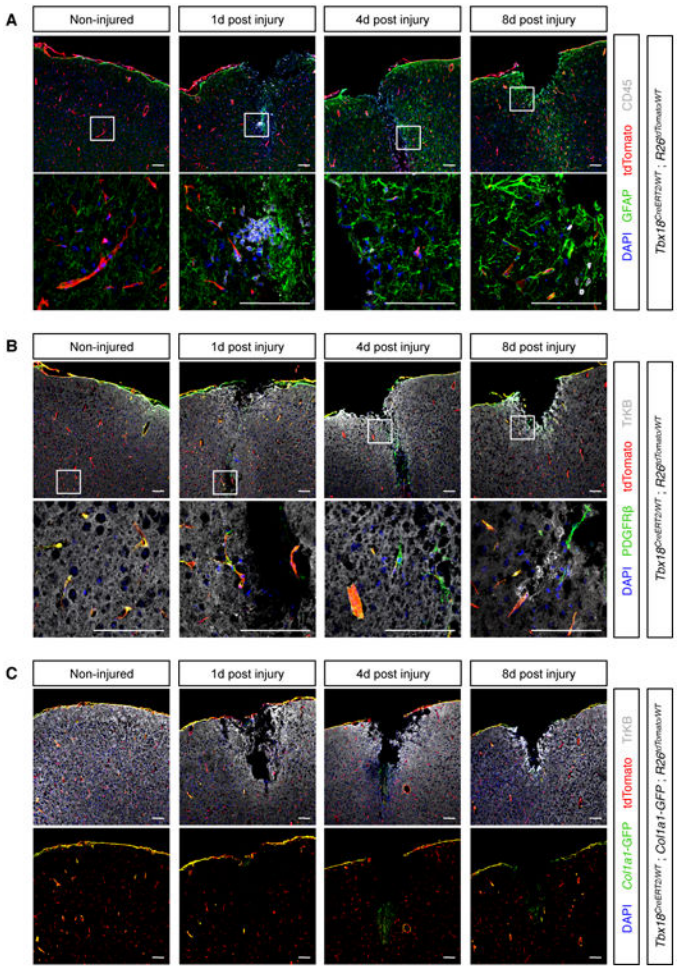


Figure 7. Pericytes of the brain were not neuronal or scar progenitors

(A) The brain responded to stab wounds by forming a glial scar mainly composed of GFAP+ reactive astrocytes (green) and CD45+ macrophages/microglia (gray). Importantly, such cells were not labeled by tdTomato, indicating they did not derive from pericytes or vascular smooth muscle. (**B**) After wounding, *Tbx18*-CreERT2 lineage traced cells never co-localized with the neuronal marker TrKB and always expressed the pan-mural cell marker PDGFRβ, indicating they retained a pericyte or vascular smooth muscle cell phenotype even after an injury setting. (**C**) In non-injured cortical tissue, *Collal*-GFP expression was restricted to specific subsets of *Tbx18+* cells: pia mater and mural cells surrounding larger vessels. Although cortical stab wounds did not produce robust fibrosis, a small number of *Collal*-GFP+ fibroblasts could be detected 4-day post injury, at the tip of the wound. However, such *Collal*-GFP+ fibroblasts were not labeled by tdTomato, indicating they did not derive from pericytes or vascular smooth muscle. Bars = 100μm.